J|A|C|S
ARTICLES
Published on Web 01/17/2007

Electronic and Magnetic Communication in Mixed-Valent and Homovalent Ruthenium Complexes Containing Phenylcyanamide Type Bridging Ligands

Muriel Fabre and Jacques Bonvoisin*

Contribution from the CEMES/CNRS, NanoSciences Group, BP 94347, 29 rue Jeanne Marvig, 31055 Toulouse cedex 4, France

Received October 10, 2006; E-mail: jbonvoisin@cemes.fr

Abstract: Four new phenylcyanamido-bridge dinuclear ruthenium complexes [{Ru(tpy)(thd)}$_2$(μ-L)] with tpy = 2,2′:6′,2″-terpyridine, thd = 2,2,6,6-tetramethyl-3,5-heptanedione and L = dcbp = 4,4′-dicyanamidobiphenyl; bcpa = bis(4-cyanamidophenyl)acetylene; bcpda = bis(4-cyanamidophenyl)diacetylene; bcpea = 9,10,-bis(4-cyanamidophenylethynyl)anthracene have been prepared and fully characterized. The mixed valent Ru(II)Ru(III) and homovalent paramagnetic Ru(III)Ru(III) forms of all the complexes were electrochemically generated and studied by UV−vis−NIR and EPR spectroscopy. Electronic communication was quantified by the electronic coupling parameter V_{ab} extracted from intervalence measurements in the near IR area, and magnetic communication was quantified in terms of the exchange coupling constant J, accessible from the intensity of the EPR signal when varying the temperature. Exponential decays for both electronic and magnetic coupling versus intermetallic distance were obtained and discussed.

1. Introduction

It is almost a truism now that, after the inception of the Creutz-Taube ion $[(H_3N)_5Ru(pyrazine)Ru(NH_3)_5]^{5+}$ in 1969,[1] studies of mixed/intermediate valence complexes and their role in intramolecular electro- and magnetocommunication have become vital parts of contemporary research in coordination chemistry.[2−6] Much effort has been invested in the elucidation of the role that the nature of the spacer between two interacting units plays in governing the redox splitting between successive electron-transfer steps (electrocommunication) and the sign and magnitude of exchange coupling of unpaired spins (magnetocommunication). The ability of the spacer to transmit electronic effects has commonly been studied by electrochemistry, using the redox splitting, i.e., the potential difference of consecutive redox steps as a measure of intramolecular intermetallic communication. One has to remember that even in the unfavorable case where this potential difference is small, leading to a single electrochemical wave a comfortable proportion of mixed valence species (>50%) exists in solution,[2] except if inversion of standard potentials occurs[7] which is not the case here. In this work, once the mixed valence species is obtained, from a practical point of view, instead of the redox splitting method, the electron-transfer process will be probed by the intensity of the intervalence transition (IT) in the NIR, according to the relation devised by N. Hush in 1967.[8] This yields the electronic coupling parameter V_{ab} describing the amount of electronic interaction between remote sites. From this interaction, one can devise general rules for the design of efficient bridging ligands allowing long-distance electron transfer. In addition, mixed-valence compounds can be simple models for the expanding domain of nanojunctions, in which a single molecule is bridging two nanoscale metallic conductors.[9] However, as the sizes of the compounds increase, synthetic problems become more acute, particularly with a decrease in free ligand solubility. In addition, the electronic coupling decreases and its detection become problematic. Thus, there is a need for new classes of compounds and/or new methods that would be more easily accessible and would exhibit or allow reaching either stronger metal−metal couplings or longer metal−metal distances than conventional systems studied so far. Some chemistry alternatives can be found by using cyclometallated complexes.[10] With increasing intermetallic distance and/or diminishing transfer abilities of the spacer, more sensitive detection methods must be applied. If the terminal groups at each extremity of the bridging ligand are paramagnetic, determination of the exchange constant J provides the information. This can be accomplished by magnetic susceptometry or EPR spectroscopy for $J \geq 1$ cm^{-1} and by EPR

(1) Creutz, C.; Taube, H. *J. Am. Chem. Soc.* **1969**, *91* (14), 3988.
(2) Launay, J.-P. *Chem. Soc. Rev.* **2001**, *30*, 386.
(3) Launay, J.-P.; Coudret, C. Wires Based on Metal Complexes. *Electron Transfer in Chemistry*; Wiley-VCH: 2001; Vol. 5, p 3.
(4) Kahn, O. *Molecular Magnetism*; Wiley-VCH: 1993.
(5) Crutchley, R. J. *Adv. Inorg. Chem.* **1994**, *41*, 273.
(6) Ward, M. D. *Chem. Soc. Rev.* **1995**, *24* (2), 121. Paul, F.; Lapinte, C. *Coord. Chem. Rev.* **1998**, *178*−*180*, 431. McCleverty, J. A.; Ward, M. D. *Acc. Chem. Res.* **1998**, *31* (12), 842. Brunschwig, B. S.; Sutin, N. *Coord. Chem. Rev.* **1999**, *187*, 233. Kaim, W.; Klein, A.; Gloeckle, M. *Acc. Chem. Res.* **2000**, *33* (11), 755. Demadis, K. D.; Hartshorn, C. M.; Meyer, T. J. *Chem. Rev.* **2001**, *101*, 2655. Ward, M. D.; McCleverty, J. A. *J. Chem. Soc., Dalton Trans.* **2002**, (3), 275.
(7) Hapiot, P.; Kispert, L. D.; Konovalov, V. V.; Savéant, J.-M. *J. Am. Chem. Soc.* **2001**, *123* (27), 6669.
(8) Hush, N. S. *Prog. Inorg. Chem.* **1967**, *8*, 391.
(9) Joachim, C.; Gimzewski, J. *Europhys. Lett.* **1995**, *30*, 409. Langlais, V. J.; Schlittler, R. R.; Tang, H.; Gourdon, A.; Joachim, C.; Gimzewski, J. K. *Phys. Rev. Lett.* **1999**, *83* (14), 2809. Rousset, V.; Joachim, C.; Rousset, B.; Fabre, N. *J. Phys. III* **1995**, *5*, 1983.
(10) Fraysse, S.; Coudret, C.; Launay, J.-P. *J. Am. Chem. Soc.* **2003**, *125* (19), 5880.

10.1021/ja067255i CCC: $37.00

Scheme 1

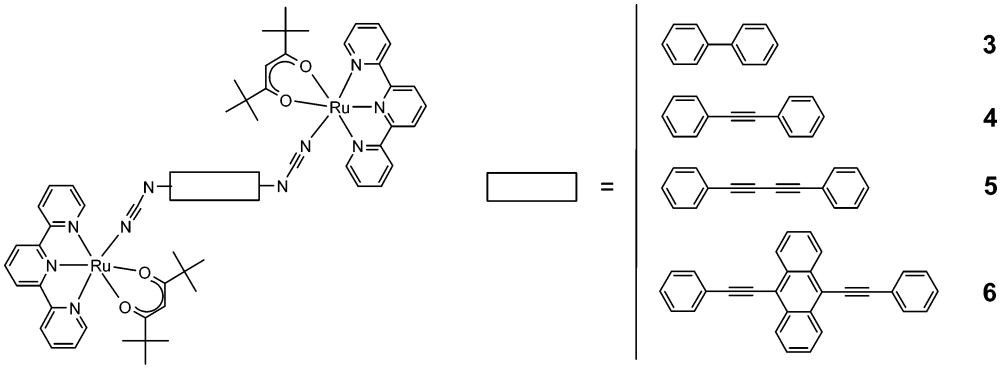

spectroscopy for much smaller J values. At this point, an important question must be addressed which is to know whether the more important phenomena of intramolecular long-distance electron transfer and energy transfer are somehow related to electron-spin exchange coupling, bearing in mind that ET is a one-electron process, whereas exchange coupling is a two-electron process. In fact, as Forbes[11] has pointed out, both processes are facets of the more general donor−acceptor interaction having in common the electron-transfer matrix element V_{ab}. The possibility of correlating J and V_{ab} has already been addressed by other authors.[5,12−17] Our own contribution to the field is to find good candidates which will allow obtaining both J (in the homovalent/isovalent paramagnetic form) and V_{ab} (in the mixed valent MV form) in order to then correlate them. The bridging ligand containing cyanamide group seems to be particularly well suited since strong interactions have been obtained in homovalent[18] or MV ruthenium complexes.[19] Following this line, few years ago, we have reported two series of dinuclear ruthenium complexes containing cyanamide derivatives as bridging ligands.[20,21] For both series, V_{ab} and J could not be obtained because of stability and/or solubility problems. Here we present the successful synthesis of four new dinuclear ruthenium complexes (see Scheme 1) with terpyridine (tpy) and bulky "acac" type ancillary ligands named thd, with four cyanamide derivatives bridging ligands with formula [{Ru(tpy)(thd)}$_2$(μ-L)] with tpy = 2,2′:6′,2″ terpyridine, thd = 2,2,6,6-tetramethyl-3,5-heptanedione, and L = dcbp = 4,4′-dicyanamidobiphenyl; bcpa = bis(4-cyanamidophenyl)acetylene; bcpda = bis(4-cyanamidophenyl)diacetylene; bcpea = 9,10,-bis(4-cyanamidophenylethynyl)anthracene. In addition, the work described here provides the first quantitative experimental comparison of the decay law for both the electronic (in the MV form) and the magnetic (in the homovalent paramagnetic form) coupling parameters versus intermetallic distance using the same family of compounds for both phenomena.

2. Results and Discussion

Synthesis. The synthesis of [Ru(tpy)(thd)(TMSepcyd)] **2** from [Ru(tpy)(thd)(Ipcyd)] **1** was adapted from literature procedures.[22] The Trimethylsilyl-protected alkyne complex [Ru(tpy)(thd)-(TMSepcyd)] **2** was prepared by a Sonogashira cross-coupling reaction between the iodoruthenium complex **1** and trimethylsilylacetylene under classic conditions ((Pd(PPh$_3$)$_2$Cl$_2$, CuI, piperidine, DMF). Complex [{Ru(tpy)(thd)}$_2$(μ-dcbp)] **3** was synthesized using a method adapted from the Suzuki cross-coupling between a halogenaryl and an arylboronic ester.[23] It is a one-pot synthesis, the arylboronic ester being generated in situ. Complex **1** was put in solution in DMF with 0.5 equiv of bis(pinacolato)diboran in the presence of PdCl$_2$dppf catalyst and K$_2$CO$_3$ as basic agent (Scheme 2). Complex [{Ru(tpy)(thd)}$_2$-(μ-bcpea)] **6** was synthesized by a Sonogashira cross-coupling reaction between the iodoruthenium complex **1** and 9,10-diethynylanthracene, which is formed in situ by deprotection of 9,10-bis(3-hydroxy-3-methylbutynyl)anthracene with potassium *tert*-butoxide (Scheme 2). Complex [{Ru(tpy)(thd)}$_2$(μ-bcpa)] **4** was synthesized by a Sonogashira cross-coupling reaction between the iodoruthenium complex **1** and the ethynylated complex [Ru(tpy)(thd)(epcyd)] formed in situ by deprotection of the trimethylsilyl-protected alkyne complex **2** with potassium carbonate, under classic conditions (Pd(PPh$_3$)$_2$Cl$_2$, CuI, piperidine, and DMF) but in the presence of a strong base such as DBU (1,8-diazabicyclo[5.4.0]undec-7-ene) given the weak reactivity of the alkyne function toward deprotonation (Scheme 3). Complex [{Ru(tpy)(thd)}$_2$(μ-bcpda)] **5** was obtained by a homo coupling reaction using the ethynylated complex [Ru(tpy)(thd)(epcyd)] formed in situ in the same way as for complex **4**. This reaction was performed with DBU and copper(I) chloride in dry pyridine with oxygen bubbling.

Electrochemistry. Cyclic voltammograms (CV) of the complexes were recorded in dichloromethane under an argon

(11) Forbes, M. D. E.; Ball, J. D.; Avdievich, N. *J. Am. Chem. Soc.* **1996**, *118*, 4707.
(12) Felthouse, T. R.; Hendrickson, D. N. *Inorg. Chem.* **1978**, *17* (9), 2636. Bayly, S. R.; Humphrey, E. R.; de Chair, H.; Paredes, C. G.; Bell, Z. R.; Jeffery, J. C.; McCleverty, J. A.; Ward, M. D.; Totti, F.; Gatteschi, D.; Courric, S.; Steele, B. R.; Screttas, C. G. *J. Chem. Soc., Dalton Trans.* **2001**, (9), 1401. Shultz, D. A.; Fico, R. M. J.; Bodnar, S. H.; Krishna Kumar, R.; Vostrikova, K. E.; Kampf, J. W.; Boyle, P. D. *J. Am. Chem. Soc.* **2003**, (125), 11761. Elschenbroich, C.; Plackmeyer, J.; Nowotny, M.; Harms, K.; Pebler, J.; Burhgaus, O. *Inorg. Chem.* **2005**, *44*, 955. Elschenbroich, C.; Plackmeyer, J.; Nowotny, M.; Behrendt, A.; Harms, K.; Pebler, J.; Burghaus, O. *Chem. Eur. J.* **2005**, *11*, 7427.
(13) Bertrand, P. *Chem. Phys. Lett.* **1985**, *113*, 104.
(14) Nelsen, S. F.; Ismagilov, R. F.; Powell, D. R. *J. Am. Chem. Soc.* **1998**, *120* (8), 1924. de Montigny, F.; Argouarch, G.; Costuas, K.; Halet, J.-F.; Toupet, L.; C., L. *Organometallics* **2005**, *24*, 4558.
(15) Brunold, T. C.; Gamelin, D. R.; Solomon, E. I. *J. Am. Chem. Soc.* **2000**, *122*, 8511.
(16) Weiss, E. A.; Ahrens, M. J.; Sinks, L. E.; Gusev, A. V.; Ratner, M. A.; Wasielewski, M. R. *J. Am. Chem. Soc.* **2004**, *126* (17), 5577.
(17) Weiss, E. A.; Wasielewski, M. R.; Ratner, M. A. *Top. Curr. Chem.* **2005**, *257*, 103.
(18) Aquino, M. A. S.; Lee, F. L.; Gabe, E. J.; Bensimon, C.; Greedan, J. E.; Crutchley, R. J. *J. Am. Chem. Soc.* **1992**, *114* (13), 5130.
(19) Rezvani, A. R.; Evans, C. E. B.; Crutchley, R. J. *Inorg. Chem.* **1995**, *34* (18), 4600. Mosher, P. J.; Yap, G. P. A.; Crutchley, R. J. *Inorg. Chem.* **2001**, *40*(6), 1189.
(20) Fabre, M. A.; Jaud, J.; Bonvoisin, J. J. *Inorg. Chim. Acta* **2005**, *358* (7), 2384.
(21) Sondaz, E.; Jaud, J.; Launay, J.-P.; Bonvoisin, J. *Eur. J. Inorg. Chem.* **2002**, 1924.
(22) Sonogashira, K.; Tohda, Y.; Hagihara, N. *Tetrahedron Lett.* **1975**, *16* (50), 4467.
(23) Nising, C. F.; Schmid, U. K.; Nieger, M.; Bräse, S. *J. Org. Chem.* **2004**, *69*, 6830.

Scheme 2. Synthesis of [{Ru(tpy)(thd)}$_2$(μ-dcbp)] **3** and [{Ru(tpy)(thd)}$_2$(μ-bcpea)] **6**

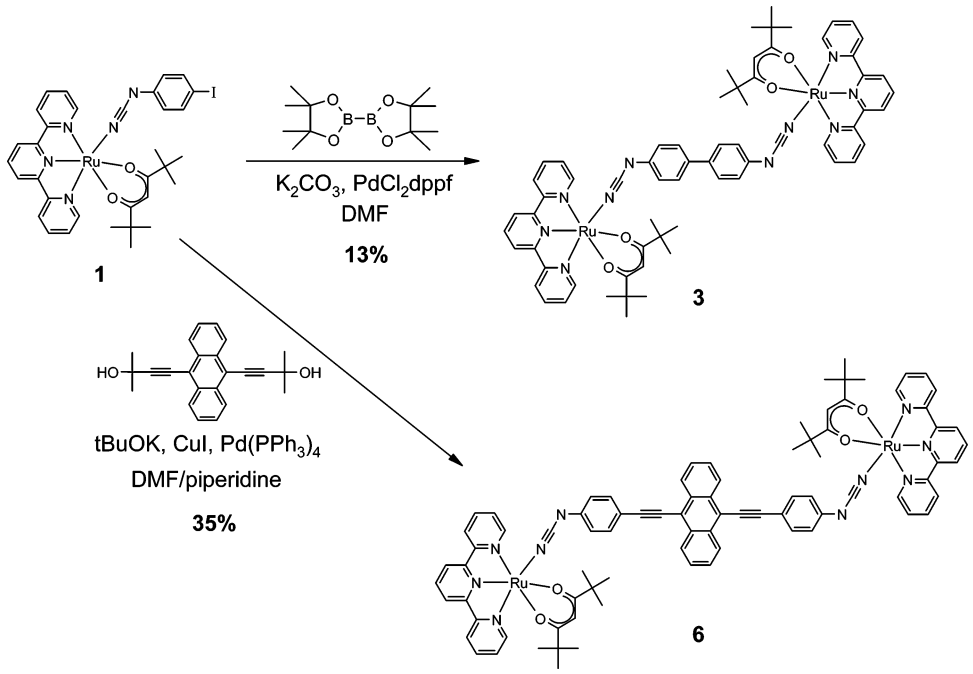

Scheme 3. Synthesis of [{Ru(tpy)(thd)}$_2$(μ-bcpa)] **4** and [{Ru(tpy)(thd)}$_2$(μ-bcpda)] **5**

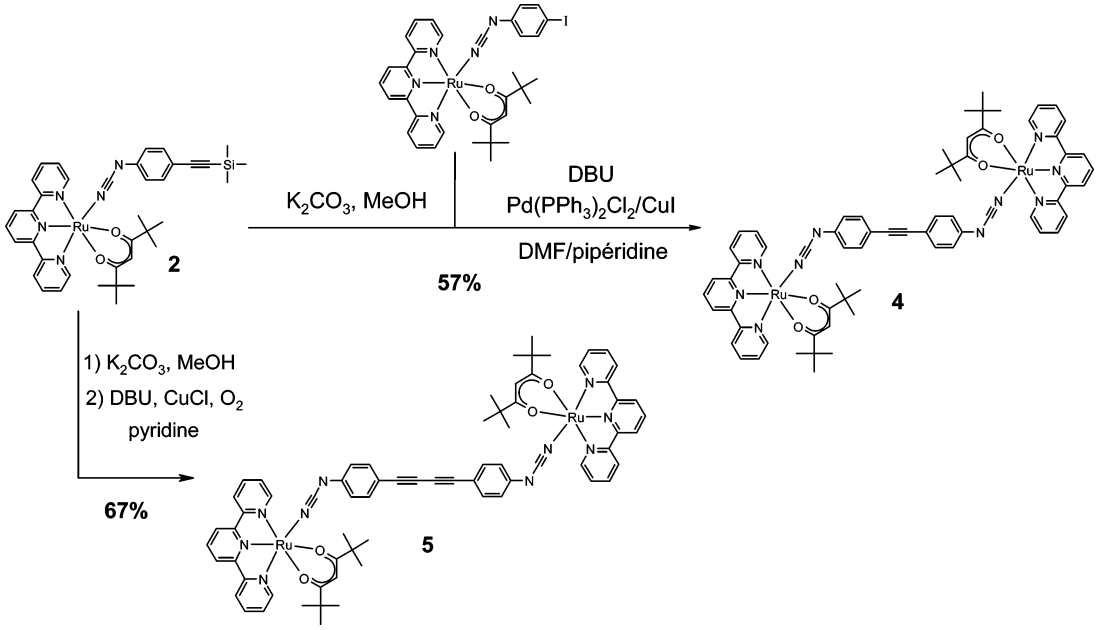

atmosphere with 0.1 M tetrabutylammonium hexafluorophosphate (TBAH) (see Figure 1 and Table 1). The $E_{1/2}$ potentials were determined from the average of the anodic and cathodic peak potentials for reversible waves. For irreversible waves, only the anodic peak potentials are reported.

In reduction, no wave was observed at least down to −1.5 V. In oxidation, several waves were observed. The first reversible wave around 0.2 V was attributed to the Ru(II/III) couple. For complexes **4**−**6**, with the longest metal−metal distance (R_{MM} = 18.5, 21.0, and 25.1 Å), the redox potentials of the ruthenium centers are too close to be distinguished, and a single bielectronic wave is then observed. One can notice that as the intermetallic distance decreases, the difference ΔE between anodic and cathodic potentials increases (from 88 mV for **6** to 108 mV for **4**). This can be explained by the increase of the energy gap between the two individual ruthenium redox potentials when the metal−metal distance decreases.

For complex **3**, which presents the shortest metal−metal distance (R_{MM} = 16 Å), ΔE is much bigger (188 mV) and one can observe a separation into two waves which corresponds to the successive oxidation of the two ruthenium centers. Differential pulse voltammetry (DPV) (see Supporting Information) was also performed in the range −0.1 to 0.4 V in order to measure the comproportionation constants K_C for complexes **3**−**6**. The results are shown in Table 2; the K_C constants were

(24) Fabre, M.; Jaud, J.; Hliwa, M.; Launay, J.-P.; Bonvoisin, J. *Inorg. Chem.* **2006**, *45* (23), 9332.
(25) Aquino, M. A. S.; White, C. A.; Bensimon, C.; Greedan, J. E.; Crutchley, R. J. *Can. J. Chem.* **1996**, *74* (11), 2201.
(26) Richardson, D. E.; Taube, H. *Inorg. Chem.* **1981**, *20* (4), 1278.

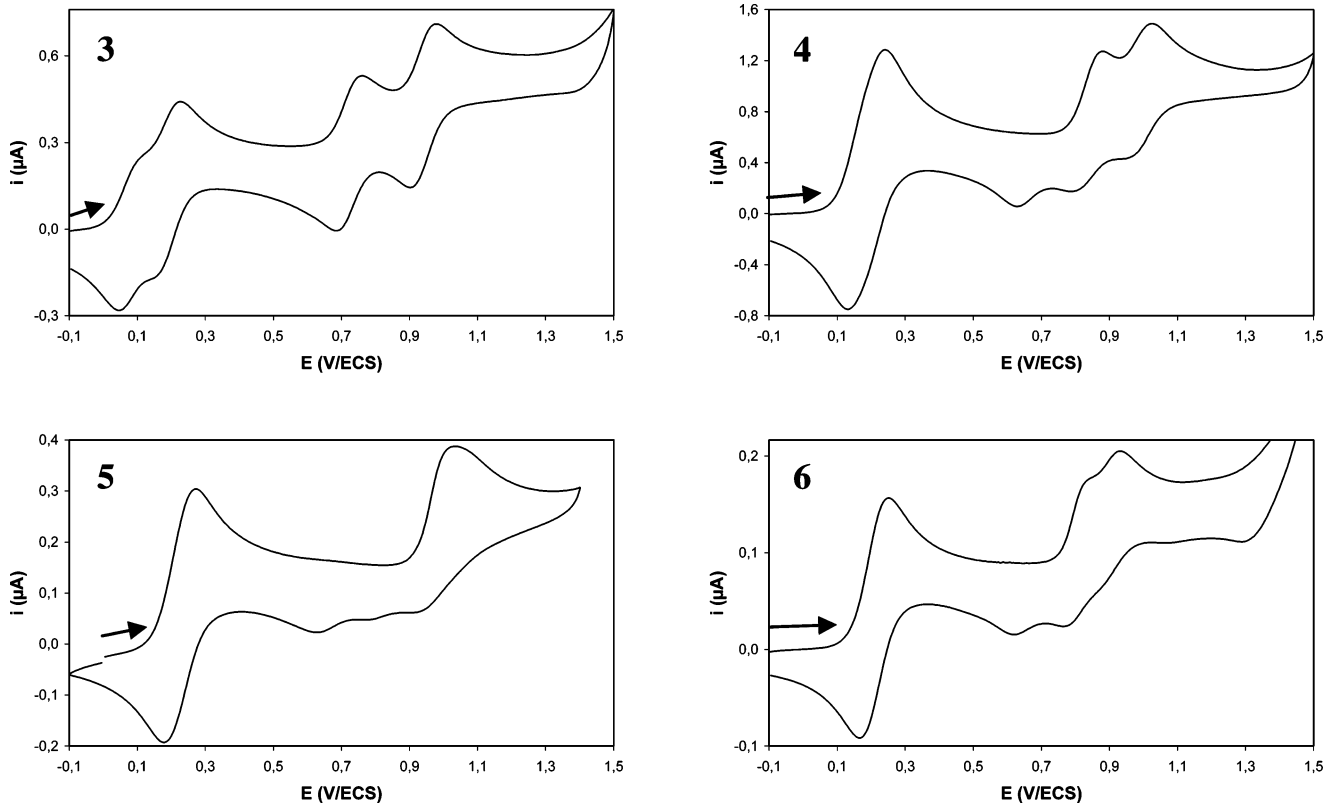

Figure 1. Cyclic voltammetry of **3**, **4**, **5**, and **6** (CH_2Cl_2, 0.1 M TBAH, 0.1 $V \cdot s^{-1}$).

Table 1. Electrochemical Data, vs ECS, in CH_2Cl_2, 0.1 M TBAH, 0.1 V/s[a]

complex	$Ru^{II/III}$ $E_{1/2}$, V (ΔE, mV)	ligand E_a (V)	ref
[Ru(tpy)(thd)Cl]	0.198 (83)	-	24
1	0.200 (78)	1.064	24
3	0.137 (180)	0.725 (78)−0.938 (73)	this work
$[\{Ru(NH_3)_5\}_2(\mu\text{-dcbp})][PF_6]_4$[b]	−0.215 (100)	0.775 (80)−0.945 (85)	25
4	0.188 (108)	0.884−1.030	this work
5	0.225 (88)	1.030	this work
6	0.211 (83)	0.764−0.930	this work

[a] $E_{1/2} = (E_a + E_c)/2$; $\Delta E = |E_a - E_c|$. E_a: anodic peak. [b] In CH_3CN.

Table 2. Oxidation Potentials and Comproportionation Constants from DPV for Complexes **3**, **4**, **5**, and **6** in DCM

complex	E°_1 (V/ECS)	E°_2 (V/ECS)	K_C
3	0.091	0.219	145 ± 5
4	0.184	0.268	26 ± 2
5	0.205	0.271	13 ± 1
6	0.184	0.234	7.0 ± 0.5

obtained by the method described by Richardson and Taube.[26] The obtained values range from $K_C = 7$ to $K_C = 145$ from the longest compound **6** to the shortest compound **3** and are quite usual for MV complexes with such metal−metal distances.

Electronic Absorption. The dinuclear compounds have been characterized by UV−vis−NIR spectroscopy in DCM (see Table 3). The spectra are comparable to those of the mononuclear and dinuclear compounds already studied with the same phenylcyanamide type ligands.[20,24]

The narrow and intense bands around 280 and 320 nm correspond to terpyridine ligand ($\pi \rightarrow \pi^*$). The larger and less intense band around 570 nm is attributable to $d\pi(Ru^{II}) \rightarrow \pi^*$-(tpy) MLCT transition. Its position and intensity are about the same for **3** to **5**, but for **6**, an intraligand transition from $bcpea^{2-}$

Table 3. UV−Vis−NIR Absorption Data of the Investigated Compounds in DCM

complex	λ_{max} in nm ($\epsilon \times 10^{-3}$ in $M^{-1} \cdot cm^{-1}$)
3	278 (73), 318 (69), 357sh (51), 578 (12)
4	278 (67), 318 (61), 386 (62), 574 (12)
5	278 (69), 318 (62), 408 (70), 570 (13)
6	270 (115), 318 (68), 344 (57), 434 (25), 552 (59)
$\mathbf{3}^{2+}$	272 (68), 312 (66), 1306 (37)
$\mathbf{4}^{2+}$	272 (69), 314 (71), 1160 (23)
$\mathbf{5}^{2+}$	272 (69), 314 (68), 1141 (29)
$\mathbf{6}^{2+}$	276 (121), 314 (65), 488 (58), 868 (17), 1234 (29)

appears in this area (344 nm) as it has already been observed in the analogous complex $[\{Ru(tpy)(acac)\}_2(\mu\text{-bcpea})]$.[20] Finally, the transitions at 357 nm for **3**, 386 nm for **4**, and 408 nm for **5** can be attributed to intraligand transitions from the bridging ligand according to the fact that they are shifted to lower energy when the conjugation of the bridge increases. Spectra of electrogenerated Ru(III)Ru(III) species are shown in Figure 2.

As previously observed for other Ru(III) complexes containing phenylcyanamide type ligand,[24] one can note the disappearance of the transition at 570 nm corresponding to the $d\pi(Ru^{II}) \rightarrow \pi^*$(tpy) MLCT transitions and the appearance of a

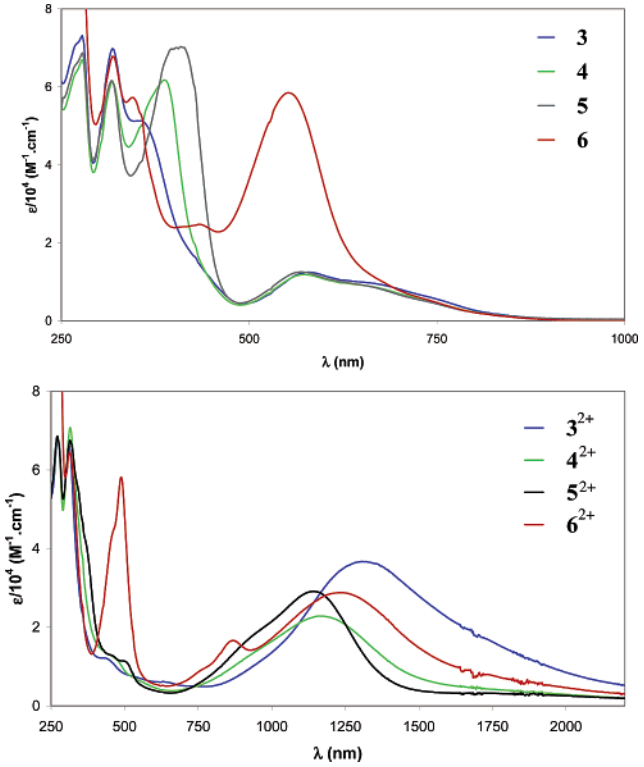

Figure 2. (Top) UV−vis−NIR spectra of **3**, **4**, **5**, and **6** in DCM. (Bottom) UV−vis−NIR spectra of $\mathbf{3}^{2+}$, $\mathbf{4}^{2+}$, $\mathbf{5}^{2+}$, and $\mathbf{6}^{2+}$ in DCM.

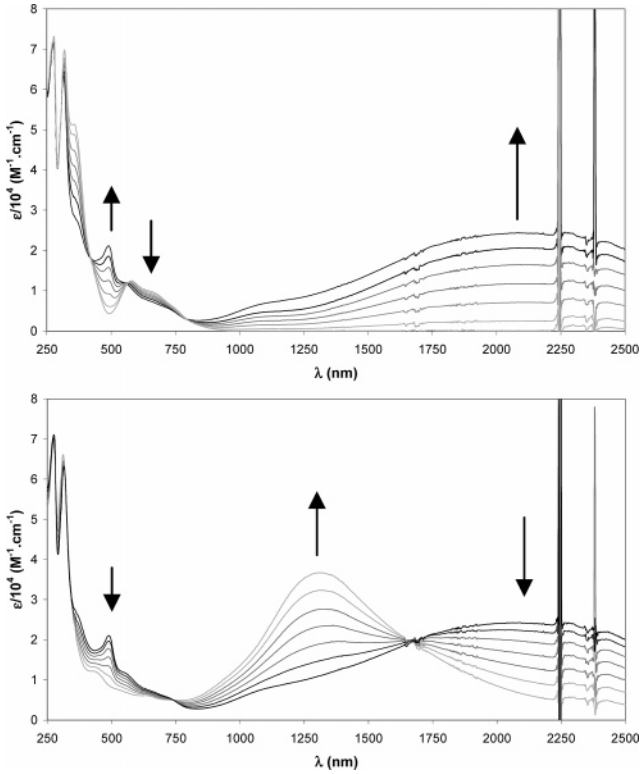

Figure 3. Spectroelectrochemical oxidation of **3** in DCM, 0.1 M TBAH (electrolysis at 0.46 V vs SCE). (Top) $\mathbf{3} \rightarrow \mathbf{3}^{+}$. (Bottom) $\mathbf{3}^{+} \rightarrow \mathbf{3}^{2+}$.

broader and more intense band in the near infrared area (1000−1500 nm) which is attributed to $\pi(\mu\text{-L}) \rightarrow d\pi(Ru^{III})$ LMCT type transition. The intensity and position of these bands vary for each studied complex, which is consistent with the attribution proposed above: LMCT transition from the bridge to the metal should be highly dependent on the structure of the bridging ligand.

Mixed Valent Species: Intervalence Transitions and Electronic Coupling. Spectroelectrochemical studies of dinuclear complexes **3**−**6** were performed in DCM. Oxidation of complexes **3**−**6** by electrolysis at controlled potential with coulommetry were followed by UV−vis−NIR spectroscopy. The electrolysis was performed at 0.46 V, which allows the oxidation of the ruthenium centers only. During the oxidation, for all four complexes, the $d\pi(Ru^{II}) \rightarrow \pi^*$(tpy) MLCT bands between 500 and 750 nm decrease in intensity and two new bands appear: The first one between 1100 and 1300 nm corresponds to a $\pi(\mu\text{-L}) \rightarrow d\pi(Ru^{III})$ LMCT transition. The second one in the near infrared area (between 1500 and 2000 nm) corresponds to a Metal to Metal Charge Transfer (MMCT) or Intervalence Transition (IT). The intensity of this band reaches a maximum at half oxidation and then decreases when the oxidation is prolonged. For the shortest complex **3**, the IT is clearly visible ($\lambda = 2078$ nm, see Figure 3). When the metal−metal distance increases (from **3** to **6**), the intensity of this transition decreases (hypochromic effect) and the IT is shifted toward shorter wavelengths (hypsochromic effect), where it is partly masked by the LMCT transition (see Table 4). Consequently, the IT becomes more and more difficult to detect and is almost undetectable for the longest complex **6** (see Supporting Information Figures S2−S4).

Table 4. Intervalence Transition Parameters and Experimental V_{ab} Values for $\mathbf{3}^{+}$, $\mathbf{4}^{+}$, $\mathbf{5}^{+}$, and $\mathbf{6}^{+}$

complex	R_{MM} (Å)	$\bar{\nu}_{max}$ (cm^{-1})	$\Delta\bar{\nu}_{1/2}$ (cm^{-1})	$\epsilon_{max} \times 10^3$ (L·mol^{-1}·cm^{-1})	V_{ab} (eV)
$\mathbf{3}^{+}$	16.0	3800 ± 300	4290 ± 300	23.9 ± 2.1	0.099 ± 0.005
$\mathbf{4}^{+}$	18.5	5020 ± 120	3910 ± 290	7.0 ± 1.0	0.051 ± 0.003
$\mathbf{5}^{+}$	21.0	5950 ± 150	3760 ± 240	3.6 ± 0.7	0.034 ± 0.002
$\mathbf{6}^{+}$	25.1	5830 ± 380	3420 ± 310	3.0 ± 1.1	0.024 ± 0.003

In order to get the electronic coupling V_{ab}, it is necessary to have the spectrum of the pure mixed valence state, i.e., once corrected from the homovalent species.[2] Because the IT appears sometimes as a shoulder or extra absorption on the longer wavelength's side, it is important to perform a deconvolution of the spectrum in order to have all the parameters (position, extinction coefficient, width) which are required to calculate the parameter V_{ab} using the Hush formula.[8,27] The deconvolutions for the four complexes are available in the Supporting Information (Figure S5). The experimental parameters of the intervalence transition for all the dinuclear complexes are gathered in Table 4.

The R_{MM} values in Table 4 were calculated taking the average of the metal−metal distance in the syn and anti conformation (see Scheme 4). In each of the conformations, the distances were evaluated using a geometry optimized structure using molecular mechanics with the Cerius2 software.[28]

In Figure 4 is illustrated the evolution of V_{ab} with metal−metal distance. The decay law was obtained using the first three values, which corresponds to the repetition of an alkyne unit: [(tpy)(thd)Ru−NCN−Ph−$(C\equiv C)_n$−Ph−NCN−Ru(tpy)(thd)] with $n = 0$, 1, or 2 for complexes **3**, **4**, or **5**, respectively. One

(27) Hush, N. S. *Coord. Chem. Rev.* **1985**, *64*, 135.
(28) *Cerius2*, 4.2; Accelrys Inc: San Diego, CA, 2000.

Scheme 4. Syn and Anti Conformations of Dinuclear Compounds

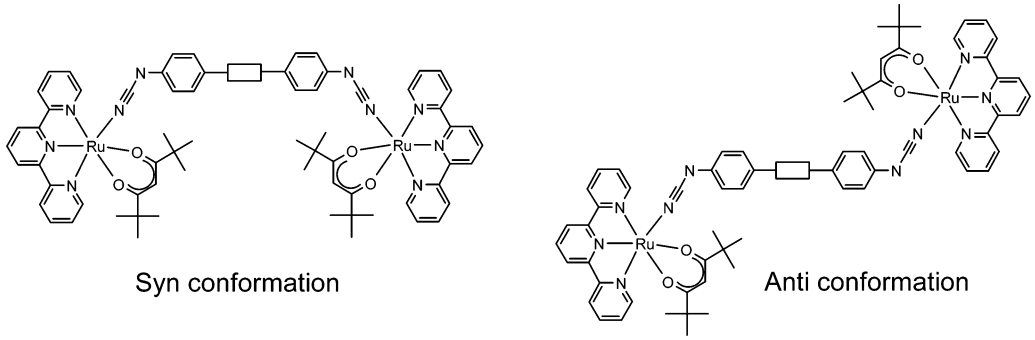

has to notice the distinction between the spacer (repeat of alkyne units) to the bridge which also includes the phenylcyanamide entity.[2] The decay of V_{ab} follows an exponential law as given by eq 1, as it has already been observed and reported elsewhere.[2,3]

$$V_{ab} = V_{ab}^{\circ} \exp(-\gamma R_{MM}) \quad (1)$$

The decay slope was found to be $\gamma = 0.21 \pm 0.03$ Å^{-1}. This value is twice or three times bigger than the one usually observed for various series (0.07−0.12 Å^{-1}).[2] This could be explained by the nature of the repeat units of the bridging ligand. By using a simple tight binding model, it has been shown that the structure of the bridge plays a crucial role on the electronic coupling.[29−31] For all the compounds in Launay's review,[2] the bridging ligands show essentially vinylene or phenylene spacers. The difference could thus be attributed to the alkyne nature of the spacer which may be less good π-connectors[32] than polyene ones or which presents some bond-length alternation effect.[33] A bigger damping factor (γ) for the acetylene bridge compared to ethylene ones was also predicted by theory.[34] This has to be nuanced due to the recent results of Crutchley et al. who showed that the decay factor is about the same for ethylene or acetylene spacers.[35] The value of V_{ab} obtained for the longest complex **6** appears to be noticeably higher than the one which would be extrapolated for the same distance with the above decay law. The peculiar role of anthracene, inserted in a molecular bridge, in mediating the electronic effect and more precisely its amplification effect has already been noticed by our group[10] and others.[14,36] Complex **6** should not follow the present series with $n = 3$, the spacer being not of the same chemical nature (anthracene vs acetylene).[2] Another alternative for the fact that compound **6**, with the anthracene bridge, does not follow the decay law would be to claim that, for such a long compound, the energy gap is comparable to the reorganization energy or electronic coupling and so superexchange and sequential mechanisms can compete. An increase in V_{ab} for **6** could be due to the dominance of an incoherent channel, namely a hopping process as it has already been evoked for charge and spin transport through para-phenylene oligomers.[16,17]

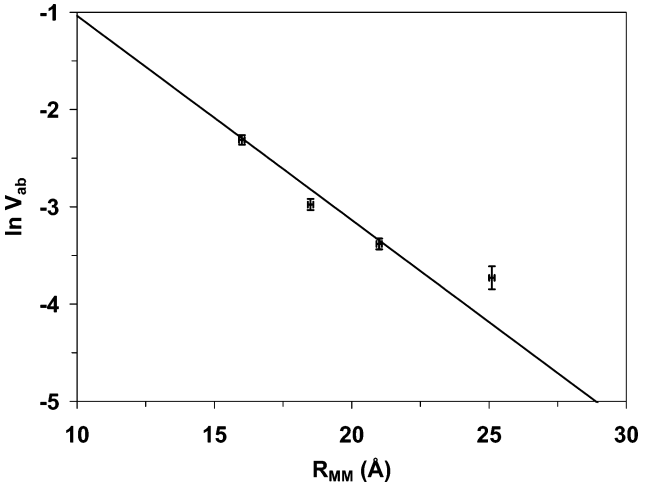

Figure 4. Decay law for the electronic coupling parameter V_{ab} in log scale vs the metal−metal distance R_{MM}.

Homovalent Species: Magnetic Coupling. The $Ru^{III}-Ru^{III}$ species were electrochemically generated. Total oxidation was checked by linear voltammetry after oxidation (see Figure S6). LV allowed us to estimate that the dinuclear compounds were oxidized up to 98%.

The EPR spectra of the oxidized species were then performed in frozen DCM solutions at 30 K (Figure 5). The spectra are quite broad, with a peak to peak separation of about 500 G, and present an anisotropic shape. The Landé factors are gathered in Table 5.

The *g* factors are in the range of 2.15 to 2.19, which is very comparable to the values obtained for $\mathbf{1}^{+}$.[24] These signals are that of an effective $S = 1$ spin state resulting from the magnetic interaction of two $S = {}^1/_2$ spin states carried by each ruthenium(III). The spectra keep the characteristics of a mononuclear ruthenium(III) $S = {}^1/_2$ spin state but with larger bandwidths. They also show a weak signal at half field, which is typical of a spin triplet and corresponds to a $\Delta M_S = 2$ forbidden transition.

To measure the magnetic coupling for each complex, EPR measurements at several temperatures can be performed.[37] In Figure 6 are reported the product of the intensity of the EPR signal times the temperature versus the temperature for the four complexes **3**−**6**. Equation 2 was used in order to extract the magnetic interaction *J*. The first term corresponds to the Bleaney

(29) McConnell, H. M. *J. Chem. Phys.* **1961**, *35*, 508.
(30) Joachim, C. *Chem. Phys.* **1987**, *116*, 339.
(31) Joachim, C.; Launay, J.-P.; Woitellier, S. *Chem. Phys.* **1990**, *147*, 131.
(32) Falgarde, F.; Katz, N. E. *Polyhedron* **1995**, *14* (9), 1213.
(33) Kushmerick, J. G.; Holt, D. B.; Pollack, S. K.; Ratner, M. A.; Yang, J. C.; Schull, T. L.; Naciri, J.; Moore, M. H.; Shashidhar, R. *J. Am. Chem. Soc.* **2002**, *124*, 10654.
(34) Magoga, M.; Joachim, C. *Phys. Rev. B* **1997**, *56* (8), 4722.
(35) Xu, G.-L.; Zou, G.; Ni, Y.-H.; DeRosa, M. C.; Crutchley, R. J.; Ren, T. *J. Am. Chem. Soc.* **2003**, *125* (33), 10057.
(36) Piet, J. J.; Taylor, P. N.; Anderson, H. L.; Osuka, A.; Warman, J. M. *J. Am. Chem. Soc.* **2000**, *122*, 1749. Taylor, P. N.; Wylie, A. P.; Huuskonen, J.; Anderson, H. L. *Angew. Chem., Int. Ed.* **1998**, *37* (7), 986. Hoshino, Y.; Suzuki, T.; Umeda, H. *Inorg. Chim. Acta* **1996**, *245*, 87.
(37) Bencini, A.; Gatteschi, D. *EPR of Exchange Coupled Systems*; Springer-Verlag: 1990; p 58.

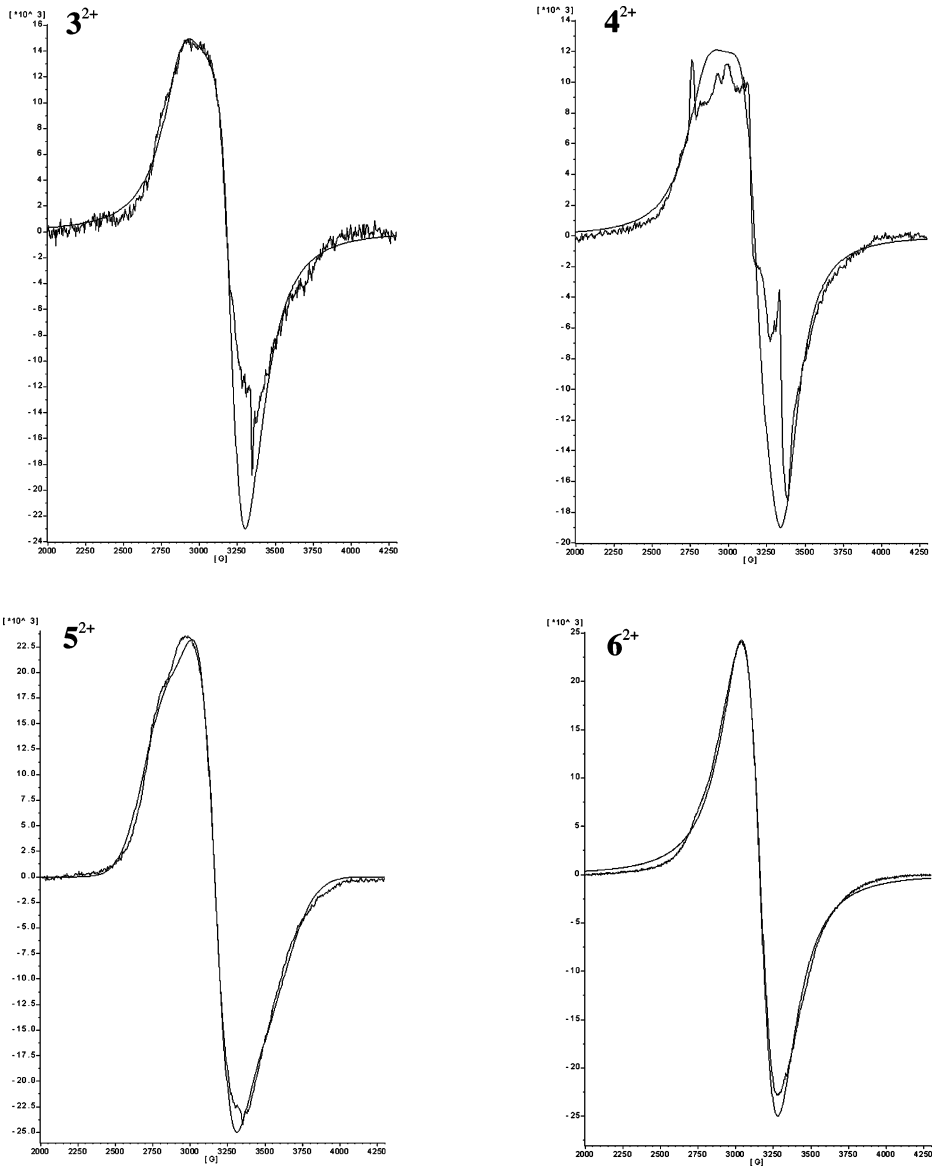

Figure 5. Experimental and simulated EPR spectrum of $\mathbf{3}^{2+}$, $\mathbf{4}^{2+}$, $\mathbf{5}^{2+}$, and $\mathbf{6}^{2+}$ in frozen DCM solution (30 K).

Table 5. EPR Parameters for $\mathbf{3}^{2+}$, $\mathbf{4}^{2+}$, $\mathbf{5}^{2+}$, and $\mathbf{6}^{2+}$ in Frozen DCM Solution (30 K)

complex	g_x	g_y	g_z	<g>
$\mathbf{3}^{2+}$	2.35	2.11	2.05	2.17
$\mathbf{4}^{2+}$	2.38	2.14	2.02	2.19
$\mathbf{5}^{2+}$	2.41	2.14	1.93	2.17
$\mathbf{6}^{2+}$	2.20	2.14	2.10	2.15

Bowers equation,[4] which describes the intramolecular interaction between two $S = {}^1/_2$ spins, and the second term takes into account the residual paramagnetism due to the presence of traces of the mixed valent species.

$$I_{\text{total}} = \frac{C_1}{T} \times \frac{1}{1 + \frac{1}{3}\exp\left(-\frac{J}{k_B T}\right)} + \frac{C_2}{T} \qquad (2)$$

All the curves shown in Figure 6 present a drop at low temperature which is characteristic of an antiferromagnetic interaction. Magnetic parameters are reported in Table 6.

One has to notice that the magnetic couplings for **3**−**6** are quite strong, from $J = -33(4)$ cm^{-1} for the shortest to $J = -13(2)$ cm^{-1} for the longest complex. No other examples of such couplings for such metal−metal distances, at least with ruthenium complexes, are found in the literature. Figure 7 shows the decay law of the magnetic coupling versus the metal−metal distance, it follows an exponential law, as given by eq 3.

$$|J| = J^\circ \exp(-\gamma' R_{\text{MM}}) \qquad (3)$$

The decay slope was found to be $\gamma' = 0.10 \pm 0.01$ Å^{-1}. It has to be noted that this decay slope is the lowest one obtained so far. In addition, one has to notice that the point corresponding to complex **6** with the anthracene unit is aligned with the three other points contrary to what was observed above for the electronic coupling. Anthracene does not seem to play a particular role for magnetic coupling or at least not as particular as for the electronic coupling!

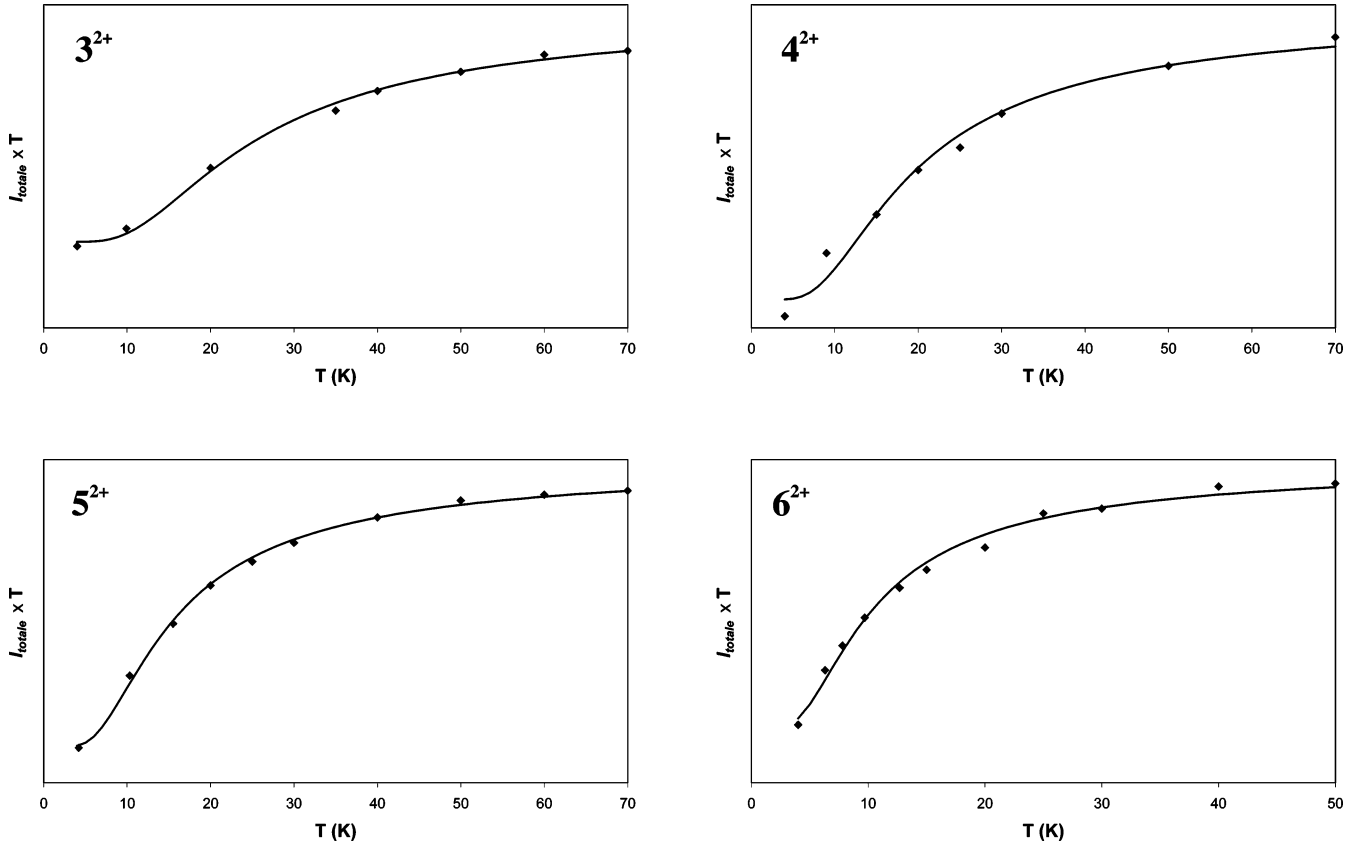

Figure 6. Double integrated EPR signal intensity times temperature ($I_{total} \times T$) of $\mathbf{3}^{2+}$, $\mathbf{4}^{2+}$, $\mathbf{5}^{2+}$, and $\mathbf{6}^{2+}$ versus temperature: experimental (dots) and simulated (lines).

Table 6. Magnetic Parameters for $\mathbf{3}^{2+}$, $\mathbf{4}^{2+}$, $\mathbf{5}^{2+}$, and $\mathbf{6}^{2+}$

complex	R_{MM} (Å)	C_1[a]	C_2[a]	J (cm^{-1})	R[b]
$\mathbf{3}^{2+}$	16.0	1.2×10^{11}	3.3×10^{10}	-33 ± 4	0.0004
$\mathbf{4}^{2+}$	18.5	5.8×10^{9}	4.2×10^{8}	-25 ± 3	0.0043
$\mathbf{5}^{2+}$	21.0	1.1×10^{11}	9.9×10^{9}	-20 ± 2	0.0003
$\mathbf{6}^{2+}$	25.1	2.2×10^{10}	3.4×10^{9}	-13 ± 2	0.0010

[a] Arbitrary units. [b] $R = \sum |I_{total} - I_{fit}|^2 / \sum I_{total}^2$.

Very few studies have been reported concerning the dependency of the magnetic interaction with intermetallic distances,[38] probably due to the difficulties of finding good objects to study. Wasielewski et al. found a slope of -0.37 Å^{-1} in a study of magnetic interactions through *p*-phenylene bridges in a series of radical pairs.[16] The nearly same value was found by Journaux et al. on dinuclear copper(II) metallacyclophanes with extended π-conjugated aromatic bridges.[39]

Comparison of the Electronic and Magnetic Coupling Parameters. We obtained two decay laws versus the intermetallic distance for the electronic coupling V_{ab} and the magnetic coupling J for the same complex series. The slopes γ and γ' are, respectively, 0.21 and 0.1 Å^{-1}. The question is to know how one can compare these two values?

A relationship between the magnetic superexchange coupling J and the electron-transfer superexchange coupling V was first developed by Kramers in 1934[40] and largely developed by Anderson in considering the magnetic properties of solid insulators.[41] Considering antiferromagnetic exchange interactions in π-stacked crystals, Soos pointed out an approximate relationship using the transition energy of charge transfer (CT) band ($h\nu_{CT}$): $J \approx V^2/h\nu_{CT}$.[42] For an intramolecular ET system, the stabilization of the adiabatic minima relative to parabolic diabatic ($V = 0$) surfaces that interact by an electronic coupling matrix element V is $-V^2/(\lambda + \Delta G°)$, where λ is the vertical

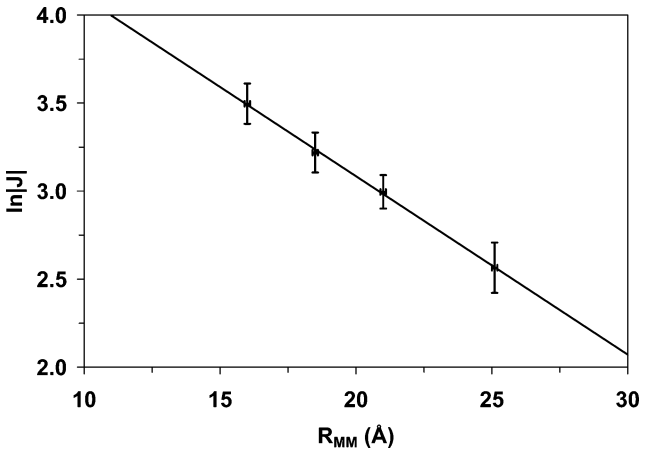

Figure 7. Decay law of the magnetic coupling versus the metal−metal distance R_{MM}.

(38) Julve, M.; Verdaguer, M.; Faus, J.; Tinti, F.; Moratal, J.; Monge, A.; Gutierrez-Puebla, E. *J. Am. Chem. Soc.* **1987**, *26*, 3520. Bürger, K.; Chaudhuri, P.; Wieghardt, K.; Nuber, B. *Chem. Eur. J.* **1995**, *1* (9), 583. Cano, J.; De Munno, G.; Sanz, J.-L.; Ruiz, R.; Faus, J.; Lloret, F.; Julve, M.; Caneschi, A. *J. Chem. Soc., Dalton Trans.* **1997**, 1915.

(39) Pardo, E.; Faus, J.; Julve, M.; Lloret, F.; Munoz, M. C.; Cano, J.; Ottenwaelder, X.; Journaux, Y.; Carrasco, R.; Blay, G.; Fernandez, I.; Ruiz-Garcia, R. *J. Am. Chem. Soc.* **2003**, *125* (36), 10770.

(40) Kramers, H. A. *Physica* **1934**, *1*, 182.

(41) Anderson, P. W. *Phys. Rev.* **1950**, *79* (2), 350. Anderson, P. W. *Phys. Rev.* **1959**, *115* (1), 2. Anderson, P. W. In *Magnetism*; Rado, G. T., Suhl, H., Eds. Academic Press: New York, 1965; Vol. 1, p 25.

(42) Soos, G. T. *Ann. Rev. Phys. Chem.* **1974**, *25*, 121.

reorganization energy and $\Delta G°$ is the free energy change for the reaction and $h\nu_{CT} = \lambda + \Delta G°$.[43] Okamura et al.[44] gave eq 4 which describes the stabilization of a diradical pair where the singlet state is stabilized by ET and the triplet is not.

$$|E(S=0) - E(S=1)| = \frac{V^2}{(\lambda + \Delta G°)} \quad (4)$$

Making the same assumption as Okamura that only the singlet is stabilized, and extending the formula toward three state system, Nelsen obtained the following eq 5:[45]

$$|E(S=0) - E(S=1)| = \frac{2V^2}{(\lambda + \Delta G°)} \quad (5)$$

Nelsen by using this equation provided the first quantitative experimental test of the relationship between J, V, and ($\lambda + \Delta G°$) based upon the properties of the +1 and +2 oxidation states of a symmetrical bis-hydrazine compound. The nearly same expression, eq 6, was given by Bertrand in studying biological molecules coupled by an exchange interaction[13,46]

$$|J_{AF}| = 2\frac{V_{ab}^2}{U} \quad (6)$$

where U represents the charge-transfer energy difference between the initial and final state at the same nuclear configuration.

In any case, one can see that J and V should follow the expression $J \approx V^2$, and then according to eqs 1 and 3, the relationship between γ and γ'should at first approximation be $\gamma' = 2\gamma$, which is almost exactly the opposite of what we observed, i.e., $\gamma' \approx \gamma/2$!

One possible explanation would be related to the specific nature of the cyanamide bridge. We have recently shown that the dicyanamidobenzene ligand, because of the close proximity in energy of its HOMO with the metal orbitals, can be a noninnocent bridging ligand.[24] Because of its ability to expand the frontier wave functions on the bridge,[47] one could think that the U term should vary with the intermetallic distance and decrease for longer bridges. Since U (eq 6) is involved in the denominator, this would explain the surprising behavior of the magnetic exchange dependence.

A more convincing explanation about the lower attenuation of J with distance could be given using the McConnell model,[29] revisited by Joachim et al.[30,31] This model cannot give quantitative values for the electronic and magnetic coupling through a given ligand, but it can give the trends when some structural parameters are varied and help in the design of efficient bridging ligands. In this model, it has been shown that when the energy difference between the metal localized states and ligand localized states is decreasing, then the damping factor (γ) is also decreasing.[31] Now, when one goes from the mixed-valent Ru(II)−Ru(III) to the iso-valent Ru(III)−Ru(III) species, there is a general decrease in metal orbital energies, and thus the energy difference between dπ(RuIII) orbitals and the HOMO of the bridging ligand is decreasing, since cyanamido type bridging ligands are known to mediate electronic and magnetic interactions through hole-transfer mechanism.[18] Thus, strictly speaking, there should be two different V_{ab} values to consider: V_{ab} for electron transfer (Ru(II)−Ru(III) situation) and V'_{ab} for magnetic interaction (Ru(III)−Ru(III) situation), of which the second one would have a lower rate of decay. This concept of two different V_{ab} values has already been introduced by Solomon et al. The authors found that V_{ab} for the MV system should be half of the iso-valent one, based on approximate calculations.[15] Nelsen et al. gave a different ratio, based on experimental measurements (1.15 instead of 2).[45] But these studies were performed on just one compound. In our case, according to the above argument on orbital energies, we should have two different V_{ab} values with different decay laws (and incidentally the V_{ab}/V'_{ab} ratio cannot stay constant with distance). With a V'_{ab} decaying more slowly with distance than V_{ab}, it is possible to explain the particularly slow decay of J_{AF} (eq 6).

This result is very encouraging since it makes the cyanamide bridging ligand a very good candidate for mediating magnetic interaction over a very long distance, since the attenuation factor is about four times lower than predicted! At this stage, quantum chemical calculations would be helpful to get insight into this interesting question. Chemical work is in progress to consolidate these results by synthesizing an even larger bridge.

3. Experimental Section

Materials. All chemicals and solvents were reagent grade or better. [Ru(tpy)Cl_3],[48] [Ru(tpy)(thd)Cl],[24] and [Ru(tpy)(thd)Ipcyd] **1**[24] were prepared according to literature procedures. Weakly acidic Brockmann I type alumina (Aldrich) was used.

Physical Measurements. UV−visible spectra were recorded on a Shimadzu UV-3100 spectrophotometer. ^{1}H and ^{13}C NMR spectra were recorded on a Bruker AMX-500 in CD_2Cl_2. IR spectra of samples in KBr pellets were taken on a Perkin-Elmer 1725 FT−IR spectrophotometer. Mass spectra were recorded by the "Service de Spectroscopie de Masse" of Paul Sabatier University using ES (Perkin-Elmer Sciex System API 365). Cyclic voltammograms were obtained with an Autolab system (PGSTAT 100) in dry dichloromethane (DCM) (0.1 M tetrabutylammonium hexafluorophosphate, TBAH) at 25 °C with a three-electrode system consisting of platinum-disk working (1 mm diameter), platinum-wire counter, and saturated calomel reference electrodes. Electrochemical oxidations were performed by electrolysis with coulometry in dry dichloromethane (0.1 M TBAH) at 25 °C at fixed potential with a three-electrode system consisting of platinum-net working, platinum-wire counter, and saturated calomel reference electrodes. Frozen solution EPR experiments were performed in DCM with a typical concentration of 5×10^{-4} M on a Bruker Elexys 500 E X-band spectrometer (equipped with a Bruker NMR Teslameter).

Synthesis of Complexes. Synthesis of [Ru(tpy)(thd)(TMSepcyd)] 2. In a Schlenk tube, [Ru(tpy)(thd)(Ipcyd)] **1** (612 mg, 0.805 mmol), CuI (26 mg, 0.14 mmol, 17 mol %), and $Pd(PPh_3)_2Cl_2$ (28 mg, 0.040 mmol, 5.0 mol %) were placed in solution in the solvent mixture DMF/piperidine (4 :1, 12 mL) previously degassed with argon. Trimethylsilylacetylene was added under argon. The reaction mixture was stirred at room temperature for 3.5 h and then evaporated to dryness. The crude was purified by column chromatography (weakly acidic alumina; solvent, dichloromethane; eluent, dichloromethane/ethanol 99.5:0.5) to give a dark blue powder of **2** (530 mg, 0.725 mmol, 90%). ES mass

(43) Sutin, N. *Prog. Inorg. Chem.* **1983**, *30*, 441.
(44) Okamura, M. Y.; Isaacson, R. A.; Feher, G. *Biochim. Biophys. Acta* **1979**, *546*, 394.
(45) Nelsen, S. F.; Ismagilov, R. F.; Teki, Y. *J. Am. Chem. Soc.* **1998**, *120* (9), 2200.
(46) Bertrand, P., Application of Electron Transfer Theories to Biological Systems. In *Structure and Bonding*; Spring-Verlag: Berlin Heidelberg, 1991; Vol. 75, p 1.
(47) Ruiz, E.; Rodriguez-Fortea, A.; Alvarez, S. *Inorg. Chem.* **2003**, *42* (16), 4881.
(48) Sullivan, B. P.; Calvert, J. M.; Meyer, T. J. *Inorg. Chem.* **1980**, *19* (5), 1404.

spectrum (CH_3CN) *m*/*z*: 732.6 $[M + H]^+$ (calcd 732.2); 546.2 [Ru(tpy)(thd)(HCN) + H]$^+$ (calcd 546.2); 518.3 [Ru(tpy)(thd)]$^+$ (calcd 518.1). ^{1}H NMR (CD_2Cl_2 $\delta = 5.35$) δ: 8.65 (2H, ddd, $J_1 = 5.5$ Hz, $J_2 = 1.6$ Hz, $J_3 = 0.8$ Hz, H_6); 8.17 (2H, ddd, $J_1 = 8.1$ Hz, $J_2 = 1.3$ Hz, $J_3 = 0.8$ Hz, H_3); 8.09 (2H, d, $J = 8.0$ Hz, $H_{3'}$); 7.88 (2H, ddd, $J_1 = 8.1$ Hz, $J_2 = 7.6$ Hz, $J_3 = 1.6$ Hz, H_4); 7.55 (1H, t, $J = 8.0$ Hz, $H_{4'}$); 7.52 (2H, ddd, $J_1 = 7.6$ Hz, $J_2 = 5.5$ Hz, $J_3 = 1.3$ Hz, H_5); 7.00 (2H, d, $J = 8.6$ Hz, H_m); 6.21 (2H, d, $J = 8.6$ Hz, H_o); 5.66 (1H, s, H_c); 1.59 (9H, s, $H_{e'}$); 0.52 (9H, s, $H_{a'}$) ; 0.24 (9H, s, H_i). ^{13}C NMR (CD_2Cl_2 $\delta = 53.48$) δ: 196.9 (C_b); 196.8 (C_d); 160.9 ($C_{2'}$); 159.6 (C_2); 154.8 (C_f); 150.7 (C_6); 135.1 (C_4); 132.3 (C_m); 126.7 ($C_{4'}$); 126.0 (C_5); 125.5 (C_{NCN}); 121.3 (C_3); 120.2 ($C_{3'}$); 118.9 (C_o); 109.7 (C_p); 107.3 (C_g); 90.3 (C_h); 88.9 (C_c); 41.6 (C_e); 40.2 (C_a); 28.7 ($C_{e'}$); 27.6 ($C_{a'}$); −0.1 (C_i). Anal. Calcd for $RuC_{38}H_{43}N_5O_2Si$: C, 62.4; H, 5.9; N, 9.6. Found: C, 62.6; H, 5.7; N, 9.5. IR ν/cm^{-1} 2179s (NCN); 2146s (C≡C).

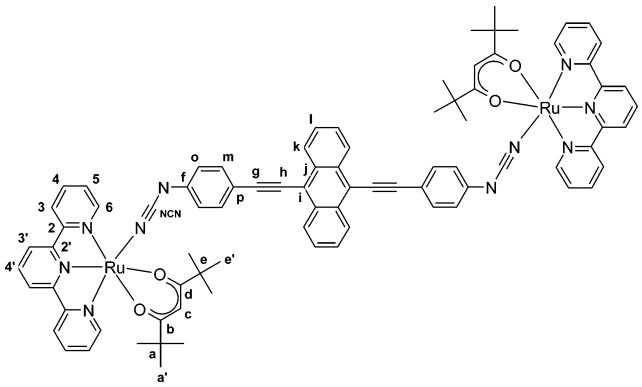

Synthesis of [{Ru(tpy)(thd)}$_2$(μ-dcbp)] 3. A Schlenk tube was charged with [Ru(tpy)(thd)(Ipcyd)] (200 mg, 0.263 mmol), potassium carbonate (109 mg, 0.789 mmol, 3.0 equiv), $PdCl_2$dppf (8.9 mg, 0.011 mmol, 4.1 mol %), and bis(pinacolato)diboron (33.4 mg, 0.132 mmol, 0.50 equiv). It was evacuated and backfilled with argon. DMF (10 mL) was added under argon, and the reaction mixture was stirred at 75 °C for 15 h. The solvent was removed under a vacuum. The crude was adsorbed on alumina and purified by column chromatography (weakly acidic alumina; solvent, dichloromethane; eluent, dichloromethane/ethanol 99:1 then 98.5:1.5). The third band (blue-green) was collected, evaporated to dryness, and dissolved in the solvent mixture dichloromethane/ethanol (4:1, 5 mL). Cyclohexane (20 mL) was added to precipitate a dark blue-green powder of **3** (22.4 mg, 0.018 mmol, 13%). ES mass spectrum (CH_3CN) m/z: 1269.3 $[M + H]^+$ (calcd 1269.4); 752.4 [Ru(tpy)(thd)(dcbpH) + H]$^+$ (calcd 752.2); 635.3 $[M + 2H]^{2+}$ (calcd 635.2); 546.2 [Ru(tpy)(thd)(HCN) + H]$^+$ (calcd 546.2); 518.3 [Ru(tpy)(thd)]$^+$ (calcd 518.1). ^{1}H NMR (CD_2Cl_2/CD_3OD, 4:1) δ: 8.63 (4H, d, $J = 5.4$ Hz, H_6); 8.20 (4H, d, $J = 8.0$ Hz, H_3); 8.11 (4H, d, $J = 8.0$ Hz, $H_{3'}$); 7.88 (4H, ddd, $J_1 = 8.0$ Hz, $J_2 = 7.7$ Hz, $J_3 = 1.2$ Hz, H_4); 7.56 (2H, t, $J = 8.0$ Hz, $H_{4'}$); 7.52 (4H, ddd, $J_1 = 7.7$ Hz, $J_2 = 5.4$ Hz, $J_3 = 1.2$ Hz, H_5); 7.04 (4H, d, $J = 8.3$ Hz, H_m); 6.33 (4H, d, $J = 8.3$ Hz, H_o); 5.65 (2H, s, H_c); 1.55 (18H, s, $H_{e'}$); 0.48 (18H, s, $H_{a'}$). ^{13}C NMR (CD_2Cl_2/CD_3OD, 4:1) δ: 197.1 (C_b); 197.0 (C_d); 161.1 ($C_{2'}$); 159.8 (C_2); 150.8 (C_6); 149.6 (C_f); 135.4 (C_4); 131.1 (C_p); 127.3 ($C_{4'}$); 126.3 (C_m); 126.2 (C_5); 124.6 (C_{NCN}); 121.5 (C_3); 120.4 ($C_{3'}$); 118.7 (C_o); 89.0 (C_c); 41.7 (C_e); 40.3 (C_a); 28.7 ($C_{e'}$); 27.6 ($C_{a'}$). Anal. Calcd for $Ru_2C_{66}H_{68}N_{10}O_4(H_2O)$: C, 61.7; H, 5.5; N, 10.9. Found: C, 61.5; H, 5.1; N, 11.2. IR ν/cm^{-1} 2163s (NCN). UV−vis−NIR CH_2Cl_2, λ in nm ($\epsilon \times 10^{-3}$ in L·mol^{-1}·cm^{-1}): 278 (73), 318 (69), 357sh (51), 578 (12). Cyclic voltammetry (CH_2Cl_2, 0.1 M TBAH, 0.1 V·s^{-1}, vs SCE): $E_{1/2}(Ru^{II}/Ru^{III}) = 0.137$ V.

Synthesis of [{Ru(tpy)(thd)}$_2$(μ-bcpa)] 4. Potassium carbonate (84 mg, 0.61 mmol, 2.1 equiv) was added to a solution of [Ru(tpy)(thd)-(TMSepcyd)] (211 mg, 0.289 mmol) in 35 mL of methanol previously degassed with argon. The mixture was stirred under argon at 40 °C for 2.5 h and then evaporated to dryness. The obtained blue residue of [Ru(tpy)(thd)(epcyd)] was used without further purification. It was dissolved in the solvent mixture DMF/piperidine (4:1, 25 mL) and added under argon to a Schlenk tube charged with [Ru(tpy)(thd)(Ipcyd)] (220 mg, 0.289 mmol), CuI (12 mg, 0.063 mmol, 22 mol %), and $Pd(PPh_3)_2$-Cl_2 (11 mg, 0.016 mmol, 5.4 mol %). DBU (91 μL, 0.608 mmol, 2.1 equiv) was added under argon to the mixture, which was stirred at room temperature for 1.5 h and then evaporated to dryness under a vacuum. The crude reaction residue was adsorbed on alumina and purified by column chromatography (weakly acidic alumina; solvent, dichloromethane; eluent, dichloromethane/ethanol 99.2:0.8 then 98.5:1.5). The compound was dissolved in the solvent mixture dichloromethane/ethanol (4:1, 50 mL), and addition of 150 mL of cyclohexane precipitated a dark green powder of **4** (213 mg, 0.165 mmol, 57%). ES mass spectrum (CH_3CN) *m*/*z*: 1293.6 $[M + H]^+$ (calcd 1293.4); 776.6 [Ru(tpy)(thd)(bcpaH) + H]$^+$ (calcd 776.2); 647.6 $[M + 2H]^{2+}$ (calcd 647.2); 546.5 [Ru(tpy)(thd)(HCN) + H]$^+$ (calcd 546.2). ^{1}H NMR (CD_2Cl_2/CD_3OD, 4:1) δ: 8.62 (4H, d, $J = 5.4$ Hz, H_6); 8.20 (4H, d, $J = 8.0$ Hz, H_3); 8.12 (4H, d, $J = 8.0$ Hz, $H_{3'}$); 7.89 (4H, ddd, $J_1 = 8.0$ Hz, $J_2 = 7.7$ Hz, $J_3 = 1.5$ Hz, H_4); 7.58 (2H, t, $J = 8.0$ Hz, $H_{4'}$); 7.52 (4H, ddd, $J_1 = 7.7$ Hz, $J_2 = 5.4$ Hz, $J_3 = 1.5$ Hz, H_5); 7.01 (4H, d, $J = 8.3$ Hz, H_m); 6.28 (4H, d, $J = 8.3$ Hz, H_o); 5.65 (2H, s, H_c); 1.55 (18H, s, $H_{e'}$); 0.49 (18H, s, $H_{a'}$). ^{13}C NMR (CD_2Cl_2/CD_3OD, 4:1) δ: 197.1 (C_b); 197.0 (C_d); 161.0 ($C_{2'}$); 159.8 (C_2); 152.0 (C_f); 150.8 (C_6); 135.5 (C_4); 131.7 (C_m); 127.5 ($C_{4'}$); 126.2 (C_5); 125.2 (C_{NCN}); 121.6 (C_3); 120.4 ($C_{3'}$); 118.5 (C_o); 112.2 (C_p); 89.0 (C_c); 88.2 (C_g); 41.6 (C_e); 40.3 (C_a); 28.7 ($C_{e'}$); 27.6 ($C_{a'}$). Anal. Calcd for $Ru_2C_{68}H_{68}N_{10}O_4$-$(H_2O)$: C, 62.4; H, 5.4; N, 10.7. Found: C, 62.4; H, 5.1; N, 10.9. IR ν/cm^{-1} 2152s (NCN). UV−vis−NIR CH_2Cl_2, λ in nm ($\epsilon \times 10^{-3}$ in L·mol^{-1}·cm^{-1}): 278 (67), 318 (61), 386 (62), 574 (12). Cyclic voltammetry (CH_2Cl_2, 0.1 M TBAH, 0.1 V·s^{-1}, vs SCE): $E_{1/2}(Ru^{II}/Ru^{III}) = 0.188$ V.

Synthesis of [{Ru(tpy)(thd)}$_2$(μ-bcpda)] 5. To a solution of [Ru-(tpy)(thd)(TMSepcyd)] (299 mg, 0.409 mmol) in 35 mL of methanol previously degassed with argon was added potassium carbonate (125 mg, 0.904 mmol, 2.2 equiv). The mixture was stirred under argon at 40 °C for 2.5 h and then evaporated to dryness to yield a blue residue of [Ru(tpy)(thd)(epcyd)], which was kept under argon and used without further purification. A three-necked round-bottom flask equipped with an adaptor connected to an oxygen source was charged with CuCl (18 mg, 0.18 mmol, 44 mol %). Pyridine (10 mL) and DBU (123 μL, 0.82 mmol, 2.0 equiv) were added, and the mixture was warmed to 40 °C and vigorously stirred while bubbling oxygen. The initially yellow solution turned green after several minutes, and the blue residue of [Ru(tpy)(thd)(epcyd)], previously prepared and dissolved in 15 mL pyridine, was added. The reaction mixture was stirred at 40 °C with oxygen bubbling. Additional reactants were added after 2 h (42 mol % of CuCl and 1.0 equiv of DBU) and after 3 h (17 mol % of CuCl and 1.0 equiv of DBU). After 4 h of stirring, the mixture was evaporated to dryness under a vacuum. The green residue was adsorbed on alumina and purified by column chromatography (weakly acidic alumina; solvent, dichloromethane; eluent, dichloromethane/ethanol 99.5:0.5 then 99:1). The second band (dark green) was collected, evaporated to dryness, and redissolved in the solvent mixture dichloromethane/ethanol (4:1, 50 mL). Addition of 150 mL of cyclohexane precipitated a dark green powder of **5** (180 mg, 0.137 mmol, 67%). ES mass spectrum (CH_3CN) *m*/*z*: 1317.7 $[M + H]^+$ (calcd 1317.4); 800.5 [Ru(tpy)(thd)-(bcpdaH) + H]$^+$ (calcd 800.2); 659.2 $[M + 2H]^{2+}$ (calcd 659.2); 546.5 [Ru(tpy)(thd)(HCN) + H]$^+$ (calcd 546.2). ^{1}H NMR (CD_2Cl_2/CD_3OD, 4:1) δ: 8.61 (4H, d, $J = 5.4$ Hz, H_6); 8.21 (4H, d, $J = 8.1$ Hz, H_3); 8.13 (4H, d, $J = 8.0$ Hz, $H_{3'}$); 7.89 (4H, ddd, $J_1 = 8.1$ Hz, $J_2 = 7.5$ Hz, $J_3 = 1.5$ Hz, H_4); 7.59 (2H, t, $J = 8.0$ Hz, $H_{4'}$); 7.52 (4H, ddd, $J_1 = 7.5$ Hz, $J_2 = 5.4$ Hz, $J_3 = 1.2$ Hz, H_5); 7.05 (4H, d, $J = 8.4$ Hz, H_m); 6.29 (4H, d, $J = 8.4$ Hz, H_o); 5.65 (2H, s, H_c); 1.54 (18H, s, $H_{e'}$); 0.48 (18H, s, $H_{a'}$). ^{13}C NMR (CD_2Cl_2/CD_3OD, 4:1) δ: 197.1 (C_b); 197.0 (C_d); 161.0 ($C_{2'}$); 159.8 (C_2); 153.9 (C_f); 150.8 (C_6); 135.5 (C_4); 133.1 (C_m); 127.6 ($C_{4'}$); 126.2 (C_5); 124.6 (C_{NCN}); 121.6 (C_3); 120.4 ($C_{3'}$);

118.6 (C_o); 109.6 (C_p); 89.0 (C_c); 82.7 (C_g); 72.2 (C_h); 41.6 (C_e); 40.3 (C_a); 28.7 ($C_{e'}$); 27.6 ($C_{a'}$). Anal. Calcd for $Ru_2C_{70}H_{68}N_{10}O_4(H_2O)_{0.7}$: C, 63.3; H, 5.3; N, 10.5. Found: C, 63.3; H, 5.3; N, 10.5. IR ν/cm^{-1} 2164s (NCN); 2135s (C≡C). UV−vis−NIR CH_2Cl_2, λ in nm ($\epsilon \times 10^{-3}$ in L·mol^{-1}·cm^{-1}): 278 (69), 318 (62), 408 (70), 570 (13). Cyclic voltammetry (CH_2Cl_2, 0.1 M TBAH, 0.1 V·s^{-1}, vs SCE): $E_{1/2}(Ru^{II}/Ru^{III}) = 0.225$ V.

Synthesis of [{Ru(tpy)(thd)}$_2$(μ-bcpea)] 6. A Schlenk tube was charged with [Ru(tpy)(thd)(Ipcyd)] (275 mg, 0.362 mmol), 9,10-bis-(3-hydroxy-3-methylbutynyl)anthracene (50.8 mg, 0.148 mmol, 0.41 equiv), CuI (17 mg, 0.089 mmol, 24 mol %), and $Pd(PPh_3)_4$ (29 mg, 0.025 mmol, 6.9 mol %). It was evacuated and backfilled with argon. The solvent mixture DMF/piperidine (5:1, 12 mL) and potassium *tert*-butoxide (81 mg, 0.72 mmol, 2.0 equiv) were added under argon. The reaction mixture was stirred under argon at 60 °C for 1.5 h, during which the color of the mixture changed from blue-green to brown-red and then to purple. The solvents were removed under a vacuum, and the crude was purified by column chromatography (weakly acidic alumina, solvent: dichloromethane, eluent: dichloromethane/ethanol 99.5:0.5 then 99:1). The obtained powder was dissolved in the solvent mixture dichloromethane/ethanol (4:1, 50 mL) and addition of cyclohexane (100 mL) gave a precipitate, which was filtered, washed with cyclohexane and diethylether, and dried under a vacuum to yield a purple powder of **6** (93.1 mg, 0.062 mmol, 35%). ES mass spectrum (CH_3CN) *m*/*z*: 1493.4 $[M + H]^+$ (calcd 1493.4); 976.3 [Ru(tpy)(thd)-(bcpeaH) + H]$^+$ (calcd 976.3); 747.3 $[M + 2H]^{2+}$ (calcd 747.2); 546.4 [Ru(tpy)(thd)(HCN) + H]$^+$ (calcd 546.2); 518.3 [Ru(tpy)(thd)]$^+$ (calcd 518.1). ^{1}H NMR (CD_2Cl_2/CD_3OD, 4:1) δ: 8.67 (4H, dd, $J_1 = 6.6$ Hz, $J_2 = 3.3$ Hz, H_k); 8.65 (4H, d, $J = 5.4$ Hz, H_6); 8.24 (4H, d, $J = 8.1$ Hz, H_3); 8.17 (4H, d, $J = 8.1$ Hz, $H_{3'}$); 7.92 (4H, ddd, $J_1 = 8.1$ Hz, $J_2 = 7.5$ Hz, $J_3 = 1.5$ Hz, H_4); 7.64 (4H, dd, $J_1 = 6.6$ Hz, $J_2 = 3.3$ Hz, H_l); 7.62 (2H, t, $J = 8.1$ Hz, $H_{4'}$); 7.56 (4H, ddd, $J_1 = 7.5$ Hz, $J_2 = 5.4$ Hz, $J_3 = 1.5$ Hz, H_5); 7.36 (4H, d, $J = 8.4$ Hz, H_m); 6.44 (4H, d, $J = 8.4$ Hz, H_o); 5.67 (2H, s, H_c); 1.57 (18H, s, $H_{e'}$); 0.50 (18H, s, $H_{a'}$). ^{13}C NMR (CD_2Cl_2/CD_3OD, 4:1) δ: 197.2 (C_b); 197.0 (C_d); 161.1 ($C_{2'}$); 159.8 (C_2); 153.7 (C_f); 150.8 (C_6); 135.6 (C_4); 132.4 (C_m); 131.7 (C_j); 127.6 ($C_{4'}$); 127.3 (C_k); 126.5 (C_l); 126.3 (C_5); 124.7 (C_{NCN}); 121.6 (C_3); 120.4 ($C_{3'}$); 118.8 (C_o); 118.3 (C_i); 111.2 (C_p); 104.6 (C_g); 89.1 (C_c); 84.6 (C_h); 41.8 (C_e); 40.3 (C_a); 28.7 ($C_{e'}$); 27.6 ($C_{a'}$). Anal. Calcd for $Ru_2C_{84}H_{76}N_{10}O_4(H_2O)$: C, 66.8; H, 5.2; N, 9.3. Found: C, 66.9; H, 5.1; N, 9.3. IR ν/cm^{-1} 2161s (NCN). UV−vis−NIR CH_2Cl_2, λ in nm ($\epsilon \times 10^{-3}$ in L·mol^{-1}·cm^{-1}): 270 (115), 318 (68), 344 (57), 552 (59). Cyclic voltammetry (CH_2Cl_2, 0.1 M TBAH, 0.1 V·s^{-1}, vs SCE): $E_{1/2}(Ru^{II}/Ru^{III}) = 0.211$ V.

Acknowledgment. The authors thank CNRS and MENRS (M.F.) for financial support, Alain Mari (LCC, Toulouse) for EPR measurements, Christophe Coudret (CEMES) for helpful discussions about synthesis, and Jean-Pierre Launay and Christian Joachim (CEMES) for fruitful advice.

Supporting Information Available: S1, differential pulse voltammetry for complex **3**, **4**, **5**, and **6** (CH_2Cl_2, 0.1 M TBAH, on rotating platinum electrode); S2, spectroelectrochemical oxidation of **4** in DCM, 0.1 M TBAH (electrolysis at 0.46 V vs SCE); S3, spectroelectrochemical oxidation of **5** in DCM, 0.1 M TBAH (electrolysis at 0.5 V vs SCE); S4, spectroelectrochemical oxidation of **6** in DCM, 0.1 M TBAH (electrolysis at 0.46 V vs SCE); S5, deconvolution of the IV transitions in the NIR area for $\mathbf{3}^+$, $\mathbf{4}^+$, $\mathbf{5}^+$, and $\mathbf{6}^+$ in DCM; S6, linear voltammetry for complex $\mathbf{3}^{2+}$, $\mathbf{4}^{2+}$, $\mathbf{5}^{2+}$, and $\mathbf{6}^{2+}$ electrochemically generated. This material is available free of charge via the Internet at http://pubs.acs.org.

JA067255I